TTP93-31
October 1993

COMMENT ON THE AVERAGE MOMENTUM OF TOP QUARKS IN THE THRESHOLD REGION. [1]

M. Jeżabek[a, b], J.H. Kühn[b] and T. Teubner[b]

[a] Institute of Nuclear Physics, Kawiory 26a, PL-30055 Cracow
[b] Institut für Theoretische Teilchenphysik,Universität Karlsruhe, 76128 Karlsruhe

Abstract

The behavior of the momentum distribution of top quarks in the threshold region is investigated. The qualitative behavior, in particular the dependence of the average momentum on the strong coupling constant can be understood from analytical calculations for the Coulomb potential. Ambiguities in the relation between the excitation curve and the top mass are addressed.

Of particular interest for top quark studies in the threshold region is the dependence of the total and the differential cross section on the strong coupling constant. Some intuition and qualitative understanding can already be gained from the predictions based on a pure Coulomb potential.

For a stable top quark of fixed mass the "effective threshold" can be associated with the location of the $1S$ resonance $\sqrt{s_{thr}} = 2m_t + E_{1S}$ with $E_{1S} = -E_{Ryd} = -\alpha^2 m_t/4$ which decreases with increasing α. The height of the resonance cross section is proportional to the square of the wave function at the origin and hence proportional to α^3, as long as the the resonances are reasonably well separated. In the limit of large Γ_t, that is far larger than E_{Ryd}, the overlapping $1S$, $2S$ ... resonances have to fill the gaps between the peaks. Since these gaps themselves increase proportional to α^2, one is left in the extreme case of large width with a cross section linear in α. Note that this corresponds to the behavior of the cross section close to but slightly above the threshold which is also proportional to α.

For realistic top masses of about 150 GeV one thus observes a behavior of the peak cross section quite close to the first power in α. Since the location of the peak itself depends on α, only the analysis of the full shape allows to extract the relevant information.

Once the threshold energy is determined experimentally, α and m_t are still strongly correlated and can hardly be deduced individually.

Therefore in a next step also the momentum distribution of top quarks has to be exploited to obtain further information. The discussion is again particularly simple for the Coulomb potential $V(r) = -\alpha/r$. The average momentum, in units of the Bohr momentum $\alpha m_t/2$, can

[1] Contributed to the Workshop on Physics at a Linear Collider, to be published in the proceedings

be written in terms of a function $f(\epsilon)$ which depends only on one variable $\epsilon = E/E_{Ryd}$ if the energy $E = \sqrt{s} - 2m_t$ is measured in terms of the Rydberg energy.

$$\langle p \rangle = \frac{\alpha m_t}{2} f(\epsilon) \tag{1}$$

For positive arguments the function f can be derived from obvious kinematical considerations.

$$f(\epsilon) = \sqrt{\epsilon} \qquad for \qquad \epsilon \geq 0 \tag{2}$$

For the discrete negative arguments $\epsilon_n = -1/n^2$ corresponding to the locations of the bound states the radial wave functions in momentum space are given [1] in terms of the Gegenbauer polynomials C_n^m

$$\psi(\vec{p}) = \frac{16\pi n^{3/2}}{(1+n^2p^2)^2} C_{n-1}^1 \left(\frac{n^2p^2-1}{n^2p^2+1} \right) Y_0^0(\theta, \varphi) \tag{3}$$

with

$$\int \frac{d\vec{p}}{(2\pi)^3} |\psi(\vec{p})|^2 = 1 \ . \tag{4}$$

Using the explicit forms of C_n^m

$$C_0^1(z) = 1, \qquad C_1^1(z) = 2z, \qquad C_2^1(z) = 4z^2 - 1 \tag{5}$$

one obtains through straightforward calculation

$$f(-1) = \frac{8}{3\pi}, \qquad f(-1/4) = \frac{16}{15\pi}, \qquad f(-1/9) = \frac{24}{35\pi} \ . \tag{6}$$

For arbitrary n one may exploit the following identity

$$C_n^1(\cos\phi) = \frac{\sin(n+1)\phi}{\sin\phi} \tag{7}$$

to derive the general result

$$f\left(-\frac{1}{n^2}\right) = \frac{8n}{(2n-1)(2n+1)\pi} \tag{8}$$

with the asymptotic behavior

$$f\left(-\frac{1}{n^2}\right) \to \frac{2}{n\pi} \ . \tag{9}$$

This in accord with the result expected from classical mechanics: For the average momentum of a particle on a closed orbit in the Coulomb potential one derives

$$\langle p^{2n} \rangle = \left(\frac{\alpha m_t}{2}\right)^{2n} \left(\frac{-E}{E_{Ryd}}\right)^n \frac{1}{2\pi} \int_0^{2\pi} d\xi \frac{(1-e^2\cos^2\xi)^n}{(1-e\cos\xi)^{2n-1}} \ . \tag{10}$$

Quantum mechanical orbits with angular momentum zero and high radial quantum numbers correspond to classical motions with excentricity $e = 1$. In this limiting case the classical expectation value is easily evaluated and for $n = 1/2$ one finds agreement with the quantum mechanical result. For small negative energies one therefore obtains the behavior $f(\epsilon) = 2\sqrt{-\epsilon}/\pi$. Significantly below threshold, however, the average momentum increases more rapidly with decreasing energy and between the $1S$ and the $2S$ state one observes an approximately linear dependence on the energy.

From these considerations the dependence of the average momentum on α (with E fixed) is easily understandable, in particular the seemingly surprising observation that well below threshold $\langle p\rangle$ decreases with increasing α. From (1) one derives for a shift in α (keeping the energy E fixed) the following shift in $\langle p\rangle$

$$\frac{\delta\langle p\rangle}{\langle p\rangle} = \left(1 - 2\frac{f'(\epsilon)}{f(\epsilon)}\epsilon\right)\frac{\delta\alpha}{\alpha} \,. \tag{11}$$

Above threshold as well as close to but below threshold $f \propto \sqrt{|\epsilon|}$. Hence $\epsilon f'/f = 1/2$ and the average momentum remains unaffected. Significantly below threshold, however, $\epsilon f'/f \approx 1$ and the factor in front of $\delta\alpha/\alpha$ becomes negative. This explains why $\langle p\rangle$ decreases with increasing α.

These results are illustrated in Fig.1. In Fig.1b we demonstrate that $\langle p\rangle$ as evaluated with the program for the Green function (solid line) coincides perfectly well with the values calculated from the analytical formula on resonance, indicated by the triangles. The prediction from classical mechanics, namely $\langle p\rangle \propto \sqrt{|\epsilon|}$ is shown by the dotted line and agrees nicely for positive and negative energies. In Fig.1a α_s is increased from 0.20 to 0.24 and $\langle p\rangle$ changes in accord with the previous discussion.

For definiteness we have chosen $m = m_t/2 = 60$ GeV for the reduced mass and $\alpha = 4\alpha_s/3$ with α_s varying between 0.20 and 0.24. To retain the stability of our numerical program $\Gamma_t = 3$ MeV has been kept non vanishing and a cut $p < m_t/2$ has been introduced. The curves demonstrate the increase of $\langle p\rangle$ by about 10% for the corresponding increase in α. The triangles mark the locations of the resonances and the expectation values for the momentum as calculated from (8).

The qualitative behavior remains unchanged for realistic QCD potentials. Predictions for different QCD potentials based on the techniques as described in [2, 6] are shown in Fig.2. These potentials correspond to different values of $\alpha_s(M_Z)$. Qualitatively the same behavior is observed as in Fig.1. In Fig.2a the top quark width has been set to an artificially small value of 0.03 GeV, in Fig.2b the realistic value of 0.3 GeV has been adopted.

An important feature is evident from Fig.2: The momentum calculated for positive energy is nearly independent from α_s and reflects merely the kinematic behavior, just as in the case of the Coulomb potential. This is characteristic for the choice of a potential [2] where the large distance behavior is fixed by phenomenology and decoupled from the short distance value of α_s.

At this point a brief discussion is in order on the relation between the top masses determined on the basis of different potentials. The perturbative two loop QCD potential has been calculated in momentum space and is fixed unambiguously for sufficiently large Q^2:

$$V\left(Q^2, \alpha_{\overline{MS}}(Q^2)\right) = -\frac{16\pi}{3}\frac{\alpha_{\overline{MS}}(Q^2)}{Q^2}\left[1 + \left(\frac{31}{3} - \frac{10}{9}n_f\right)\frac{\alpha_{\overline{MS}}(Q^2)}{4\pi}\right] \tag{12}$$

with

$$\begin{aligned} \frac{\alpha_{\overline{MS}}(Q^2)}{4\pi} &= \frac{1}{b_0 \log\left(Q^2/\Lambda^2_{\overline{MS}}\right)}\left[1 - \frac{b_1}{b_0^2}\frac{\log\log\left(Q^2/\Lambda^2_{\overline{MS}}\right)}{\log\left(Q^2/\Lambda^2_{\overline{MS}}\right)}\right] \\ b_0 &= 11 - \frac{2}{3}n_f, \qquad b_1 = 102 - \frac{38}{3}n_f \end{aligned} \tag{13}$$

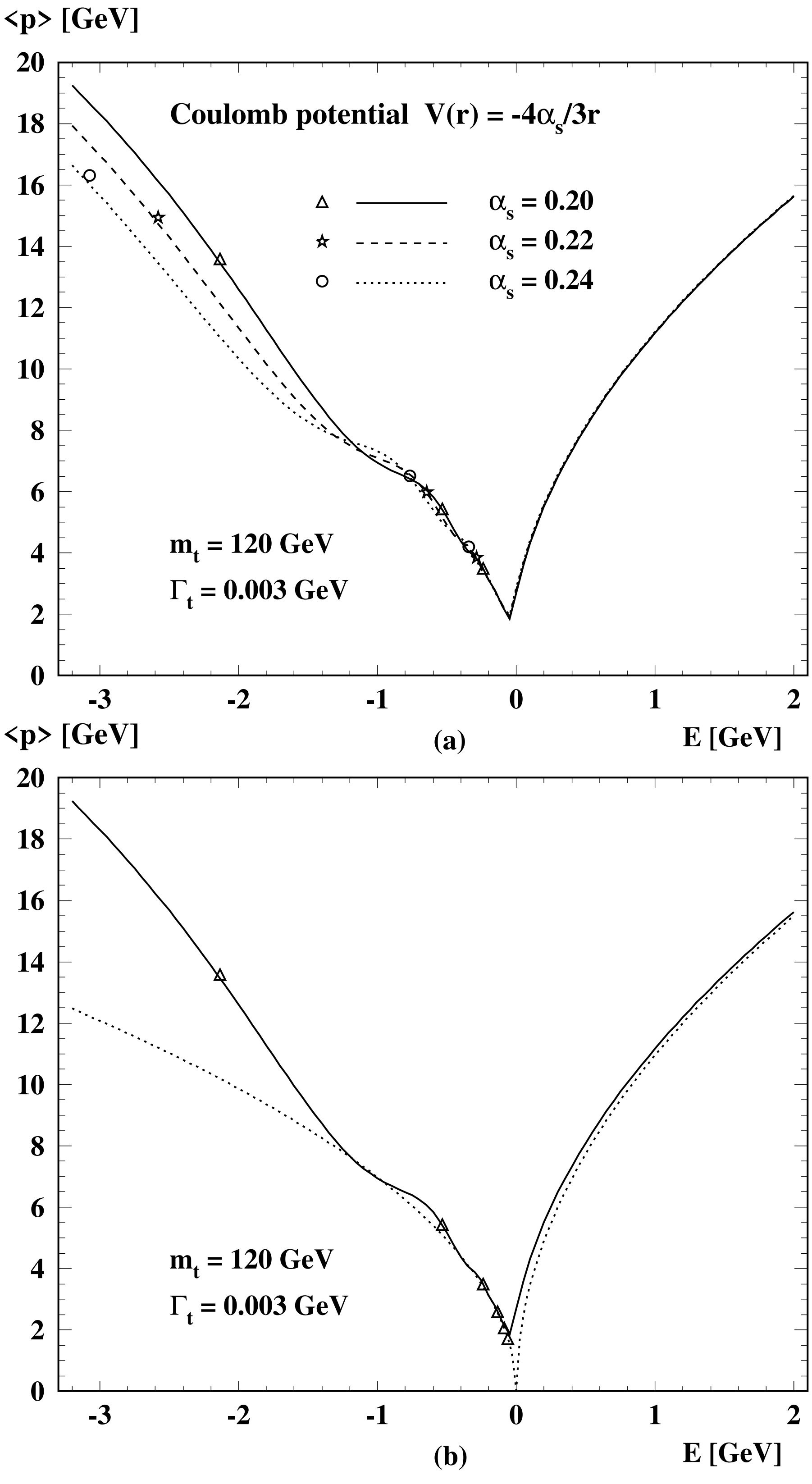

Figure 1: a) Average momentum as a function of E for different values of α. The markers show the results of the analytical calculation at $1S$, $2S$, $3S$ energies. b) Comparison with the analytical result for discrete energies and with the square–root dependence close to threshold.

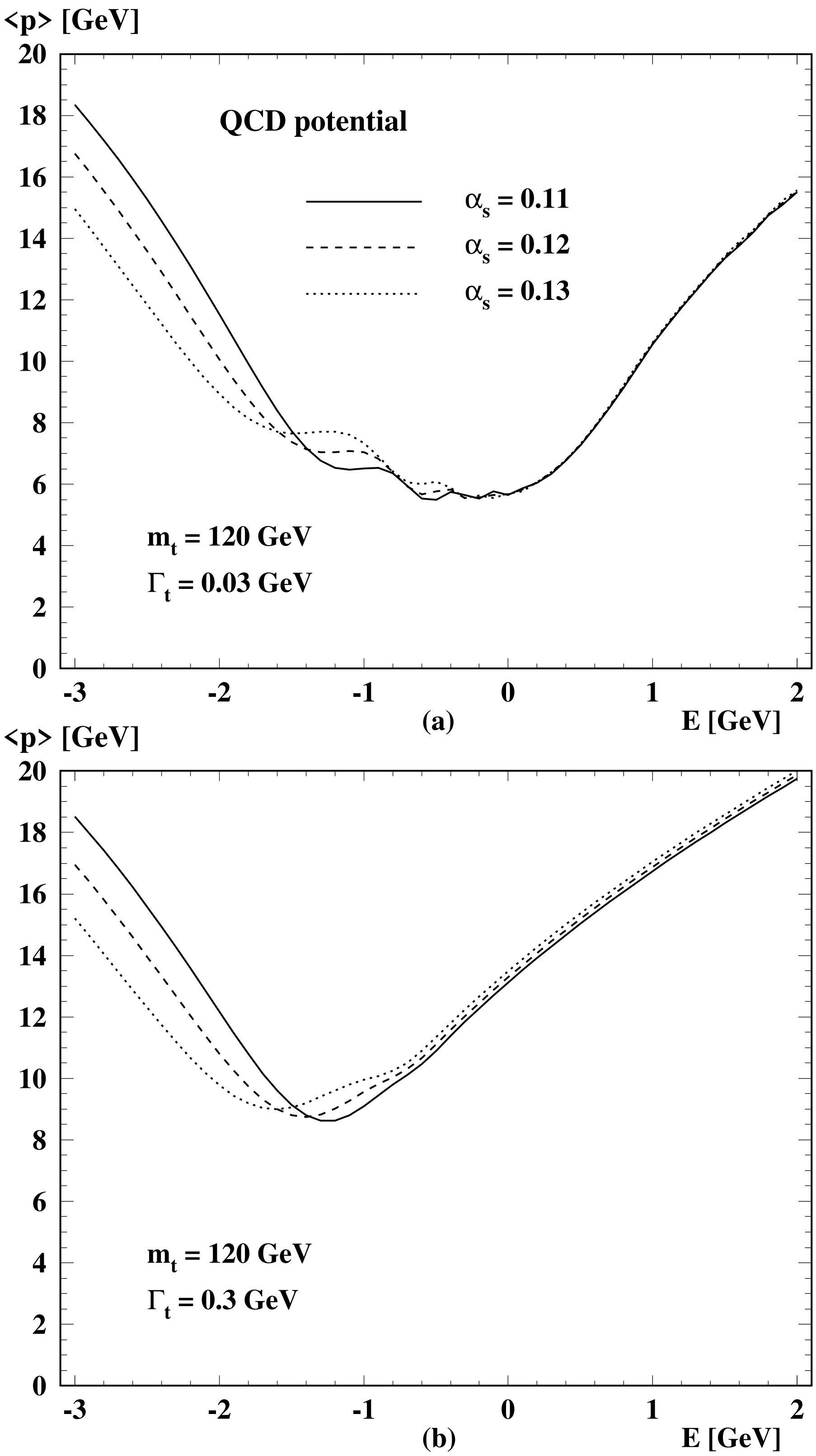

Figure 2: Energy dependence of $\langle p \rangle$, the average t quark momentum for $\alpha_s = 0.13$ (dotted) 0.12 (dashed) and 0.11 (solid) line for $m_t = 120$ GeV. a) $\Gamma_t = 0.03$ GeV and b) $\Gamma_t = 0.3$ GeV.

Power law suppressed terms cannot be calculated in this approach. To evaluate the Fourier transform of this function in order to calculate the potential in coordinate space the small Q^2 behavior has to be specified in an ad hoc manner. Different assumptions will lead to the same short distance behavior. The potentials will, however, differ with respect to their long distance behavior. In [3] it has been argued convincingly that the long distance tail is cut off by the large top width. However, an additive constant in coordinate space can be induced by the small momentum part of $\tilde{V}(Q^2)$. This additional term would lead to a shift in the $t\bar{t}$ threshold, which in turn can be reabsorbed by a corresponding shift in m_t. The different assumptions on the long distance behavior are reflected in differences between the predictions of [4, 5, 6] for the precise location of the $t\bar{t}$ threshold for identical values of α_s and m_t and in differences in the α_s dependence of the momentum distributions for fixed m_t and energy (see also [7]). All these differences can be attributed to the freedom in the additive constant discussed before. The same additive constant appears in $b\bar{b}$ spectroscopy, such that the mass difference between top and bottom is independent from these considerations.

References

[1] H.A. Bethe and E.E. Salpeter, *Quantum Mechanics of One– and Two–Electron Atoms* (Plenum Publishing Corporation, New York, 1977)

[2] M. Reżabek and T. Teubner, *Z. Phys.* **C 59** (1993) 669

[3] V.S. Fadin, V.A. Khoze, *JETP Lett.* **46** (1987) 525, *Sov. J. Nucl. Phys.* **48** (1988) 309

[4] J.M. Strassler and M.E. Peskin, *Phys. Rev.* **D 43** (1991) 1500

[5] Y. Sumino, K. Fujii, K. Hagiwara, H. Murayama, C.-K. Ng, *Phys. Rev.* **D 47** (1992) 56

[6] M. Reżabek, J.H. Kühn and T. Teubner, *Z. Phys.* **C 56** (1992) 653

[7] P. Igo–Kemenes, M. Martinez, R. Miquel, S. Orteu, contribution to this workshop